Istituto Nazionale di Ricerca Metrologica - INRiM

E. Biolcati, A. Germak, F. Mazzoleni, C. Origlia, S. Palumbo, F. Vitiello

Absolute measurements of the free-fall acceleration in Walferdange, Luxembourg ICAG 2013

Technical Report RT-15/2016 (April)

Abstract

The described work was carried out on November 2013 by the Istituto Nazionale di Ricerca Metrologica (INRiM) of Turin (Italy), for the participation fo the IX International Comparison of Absolute Gravimeters ICAG-2013 in the Underground Laboratory for Geodynamics in Walferdange, Luxembourg, organized by the University of Luxembourg.

The experimental results of the absolute measurement of the free-fall acceleration g in the three sites dedicated to the comparison are reported. The measurements were performed with the transportable absolute gravimeter IMGC-02 of the INRIM. At the same time, 25 other absolute gravimeters coming for different parts of the world enjoined to the comparison. In the proximity of the measurement sites, a super-conductor relative gravimeter was enabled, in order to monitor the variation of the gravitation field along the days.

With the IMGC-02 instrument a relative accuracy of few parts in 10^9 is reachable, i.e. measurement of g with uncertainty of tens microgals (1 μGal $= 1 \times 10^{-8}$ m s^{-2}).

$\sim \cdot \sim$

Il lavoro qui descritto è stato svolto nel mese di novembre del 2013 dall'Istituto Nazionale di Ricerca Metrologica (INRiM), per partecipare al IX Confronto Internazionale dei Gravimetri Assoluti (ICAG-2013).

Si riportano i risultati sperimentali della misura assoluta dell'accelerazione locale di gravità g nei tre siti dedicati per il confronto. Le misure sono state realizzate con il gravimetro assoluto trasportabile IMGC-02 dell'INRIM. Contemporaneamente, altri 25 gravimetri provenienti da diverse parti del mondo sono stati utilizzati per il confronto. In prossimità dei siti di misura, era attivo un gravimetro relativo super-conduttore per controllare le variazioni del campo gravitazionale giorno per giorno.

Con l'IMGC-02 si raggiunge un'accuratezza relativa di qualche parte in 10^9*, ovvero misure di g con incertezza di decine di microgal (1* μ*Gal* $= 1 \times 10^{-8}$ *m s*$^{-2}$*).*

Contents

1 IMGC-02 absolute gravimeter 5

1.1 Operating principle 5

1.2 Uncertainty 6

2 Experimental results 9

2.1 Measurement site 9

2.1.1 Site B5 9

2.1.2 Site C2 13

2.1.3 Site C3 16

3 Conclusion 19

References 20

List of Tables

1 Experimental results at the site B5. 11

2 Instrumental uncertainty of the IMGC-02. Drag, out gassing, magnetic and electrostatic field, air gap modulation, refraction index, fringe timing and radiation pressure are negligible for the budget uncertainty (1 μGal = 1×10^{-8} m s^{-2}). 12

3 Final uncertainty for the absolute measurement at the site B5. Floor recoil effect and polar motion correction (0.8 μGal) are negligible for the budget uncertainty. Data taken during the first night are used only. 12

4 Experimental results at the site C2. 14

5 Final uncertainty for the absolute measurement at the site C2. Floor recoil effect and polar motion correction (0.8 μGal) are negligible for the budget uncertainty. 15

6 Experimental results at the site C3. 17

7 Final uncertainty for the absolute measurement at the site C3. Floor recoil effect and polar motion correction (0.8 μGal) are negligible for the budget uncertainty. 18

List of Figures

1 Layout of the IMGC-02 absolute gravimeter. 6

2 Experimental results for the absolute measurements at the site B5. All and averaged values of g (minus a nominal value for visibility) versus launch number (top). Distribution of the those values with Gaussian fit superimposed and averaged residuals from the fit function to the trajectories (bottom). 10

3 Experimental parameters using for the absolute measurements at the site B5. Barometric pressure and ambient temperature values versus the launch number. 10

4 Experimental results for the absolute measurements at the site C2. All and averaged values of g (minus a nominal value for visibility) versus launch number (top). Distribution of the those values with Gaussian fit superimposed and averaged residuals from the fit function to the trajectories (bottom). 13

5 Experimental parameters using for the absolute measurements at the site C2. Barometric pressure and ambient temperature values versus the launch number. 15

6 Experimental results for the absolute measurements at the site C3. All and averaged values of g (minus a nominal value for visibility) versus launch number (top). Distribution of the those values with Gaussian fit superimposed and averaged residuals from the fit function to the trajectories (bottom). 16

7 Experimental parameters using for the absolute measurements at the site C3. Barometric pressure and ambient temperature values versus the launch number. 18

1 IMGC-02 absolute gravimeter

1.1 Operating principle

The absolute measurement of the free-fall acceleration, g, was performed with the prototype apparatus developed by INRiM [1, 2]. The g value is measured by tracking the vertical trajectory of a test-body subjected to the gravitational acceleration. The IMGC-02 adopts the symmetric rise and falling method, where both the rising and falling trajectories of the test-body are recorded. The raw datum consists in an array where each element represents the time correspondent to the passage of the test-body through equally spaced levels (or stations). A model function is fitted to the raw datum in a least-squares adjustment. One of the parameters of the model is the acceleration experienced by the test-body during its flight. A measurement session consists of about 1500 launches taking during about 10 hours, in order to be able to reduce the effect of the very low frequency Earth oscillations. The measurement session is carried out during the night to have the minimum human noise effect.

A schematic layout of the apparatus is shown in figure 1. The main parts of the instrument are a Mach-Zehnder interferometer [3] and a long-period (about 20 s) seismometer. The wavelength of a iodine stabilised He-Ne laser is used as the length standard. The inertial mass of a seismometer supports a cube-corner reflector, which is the reference mirror of the interferometer. The moving mirror of the interferometer is also a cube-corner retro-reflector and is directly subjected to the free falling motion. It is thrown vertically upwards by means of a mechanical launch pad in a vacuum chamber. Interference fringes emerging from the interferometer are detected by a photo-multiplier. The output signal is sampled by a high-speed waveform digitizer synchronized to a Rb oscillator. It is used as the time standard. Equally spaced stations are selected by counting a constant integer number of interference fringes N_f. Thus consecutive stations are separated by a distance $d = N_f \lambda/2$, being λ the wavelength of the laser radiation.

The so called *local fit method* is used to time the interference signal [4]. The time is computed by fitting the equation model of the interference of monochromatic waves to the interference fringe correspondent to the selected station. The space-time coordinates are processed in a least-squares algorithm, where a suitable non linear model function is fitted to the trajectory. Each throw gives an estimate of the g value.

A dedicated computer manages the instrument. The pad launch is triggered when the system is found to be ready. The software checks the pad launch state (loaded or unloaded) and the laser state (locked or unlocked). Environmental parameters such as the local barometric pressure and the temperature are acquired and stored for each launch.

The software includes the manager `GravisoftM` for driving the instrument and storing the measurement data and the post-processing `GravisoftPP` to analyse the data-files. These programs were developed and tested on the LabVIEW® platform.

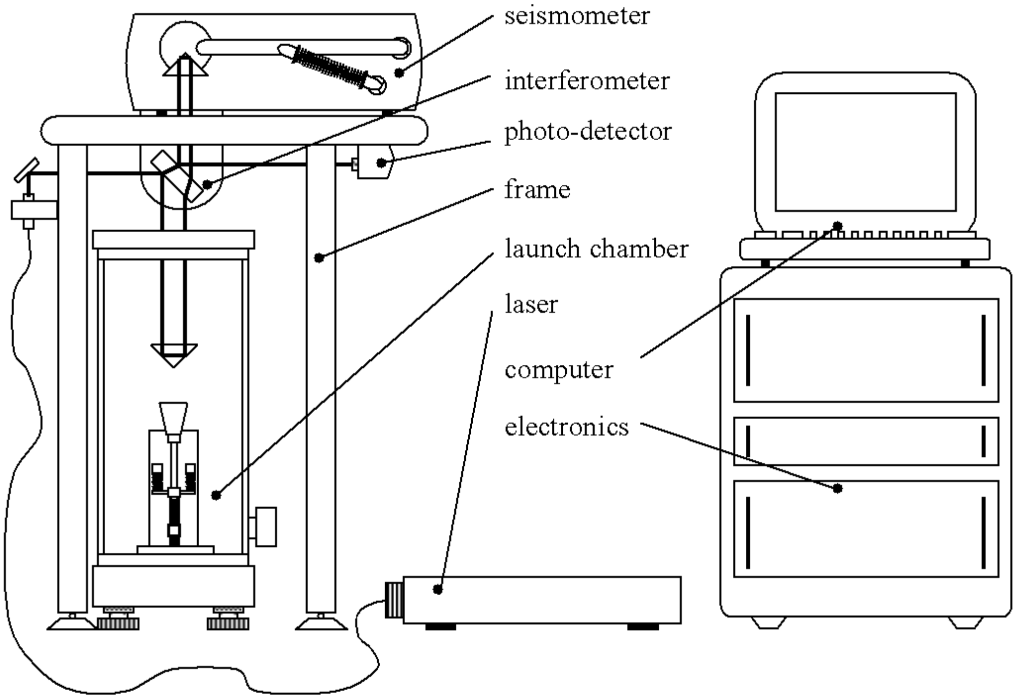

Figure 1: Layout of the IMGC-02 absolute gravimeter.

Geophysical corrections are applied: (i) the Earth tides and ocean loading are computed with the ETGTAB® (version 3.10 19950123 Fortran 77); (ii) the polar motion correction is computed starting from the daily pole coordinates x and y (rad) obtained from the International Earth Rotation Service (IERS). The gravitational acceleration is normalized to a nominal pressure. Instrumental corrections are also applied as the laser beam verticality and the laser beam divergence.

The g value associated to every measurement session is calculated as the mean of N measurements and it is referred to a specific height from the floor h_{ref}. The measurement expanded uncertainty is evaluated according to the method of combination of uncertainties as suggested by the ISO GUM guide [5].

1.2 Uncertainty

The uncertainty associated to the g measurement is evaluated by combining the contributions of uncertainty of the IMGC-02 absolute gravimeter, called *instrumental uncertainty* to the contribution of uncertainty depending on the observation site [1].

Instrumental uncertainty Influence factors which are characteristic of the instrument and are not negligible with the actual performances are listed in the following.

- *Temperature gradient.* A temperature gradient ΔT of the residual air generates a pressure gradient on the test body. The consequent acceleration coming by the ideal gas law is $a_{\text{temp}} = \Delta T\, P\, A/(T\, m)$ where A is the section of the test body.

- *Self attraction.* The mass of the parts constituting the apparatus (such as seismometer, structure, vacuum chamber, etc.) are sources of a gravitational field, which can systematically perturb the motion of the flying object. The acceleration generated by each part of the instrument is given by $a_{\text{mass,i}} = G\, M_i/z_i^2$ with G the universal gravity constant, M_i the mass of the part i, z_i the distance between the centre-of-mass of the part i and the test object at its measurement height [6].

- *Laser beam verticality.* A residual angle ϑ between the laser beam and the vertical direction modifies the value of g as follows (approximation for small angles is used): $\Delta g/g \simeq \vartheta^2/2$. The bias is then systematically negative and proportional to the square of the misalignment angle value. The probability distribution function (PDF) of such error is not centred at zero, due to the complexity of the system. For this reason, a correction for this error should be taken into account in the calculation of the final value.

- *Laser accuracy.* Each laser has a proper uncertainty associated to the accuracy of the frequency. On the other hand, the time stability of this accuracy has to be analyse too in order to check for any possible drift effect.

- *Laser beam divergence.* A Gaussian laser beam has a non-zero curvature of wave fronts. It leads to systematic biases similar to those arising from the non-verticality. When the wave fronts is curved, only the axis of the beam can be aligned on a interferometer. The remaining parts of the beam are inherently misaligned, changing the effective wavelength λ value which could require a dedicated correction as: $\Delta g/g = \Delta\lambda/\lambda \simeq \lambda^2/(4\pi^2\omega_0^2)$ where ω_0 is the waist.

- *Clock delay.* The Rb oscillator was calibrated using the Cs oscillator of the INRiM. However, the associated uncertainty and the time drift effect must be considered.

- *Retro-reflector balancing.* The dynamic equations of the test body are referred to its centre-of-mass, while the experimental trajectory is tracked relates to the optical centre of the corner-cube prism. If rotations occur during the flight, the trajectory accuracy is affected by a systematic bias related to the distance d between the two centres. The parasitic acceleration is given by: $a_{\text{cen}} = \omega^2\, d$ where ω is the angular velocity of the object.

- *Reference height.* Each launch statistically reaches a different maximum height. As a consequence, the height whose the g value is referred changes time by time. A mean value is given as reference height and the uncertainty associated on g is calculated.

Other factors as vacuum level, non-uniform magnetic field, electrostatic attraction, overall drift, air gap modulation, length and time standards and radiation pressure were studied in details and they are found to be negligible with a respect to the main effects.

Table 2 reports the quantitative assessment of effects and corrections described above. The expanded uncertainty at the 95% confidence level (coverage factor k = 2.1 and 19 degrees of freedom) is estimated to be $U = 7.9\ \mu$Gal.

Site-dependent uncertainty The main factors depending from the observation site are the following ones.

- *Coriolis force.* Each object moving relative to the Earth is subjected to the Coriolis acceleration, described as: $a_{\mathrm{Cor}} = 2\,\omega_E\,v_{EW}\ \sin(\pi/2 - \varphi)$, where ω_E is the Earth angular velocity, v_{EW} the velocity induced by the Coriolis effect, φ the latitude of the measurement site.

- *Barometric pressure.* Each g value is normalized to a nominal pressure: $\Delta g = f_B(P_{\mathrm{obs}} - P_{\mathrm{nom}})$ with $P_{\mathrm{nom}} = 1013.25(1 - h_m/44330.77)^{5.2559}$. P_{obs} is the pressure value measured during the measurement session, $f_B = 0.30\ \mu\mathrm{Gal}\cdot$ mbar is a barometric factor recommended by IAG 1983 and h_m the topographic elevation of the site.

- *Tide and ocean loading.* The gravity tide effect and the consequent ocean loading give the highest correction to each g value. However, the ETGTAB software allows a very detailed description of such effect with well known uncertainty contribution.

- *Standard deviation of the mean.* The standard deviation takes into account all the statistic contributions. In particular the low frequency oscillation effect which are not filtered by the seismometer is significantly reduced.

Floor recoil effect and the polar motion correction give an uncertainty contribution which results to be negligible for our purposes. In table 3 all the contributions are summarized for the observation sites of this technical report. Usually, for sites as dedicated laboratories with very stable floor, the final expanded uncertainty combined with the instrumental one is less than 9 μGal.

2 Experimental results

2.1 Measurement site

The site used for the comparison is the Underground mine in Walferdange. The room in which the instrument were installed is conditioned and about 300 m far from the entrance. For this reason the human noise is significantly reduced both during the day and night. However, the best measurements were performed during the night, because during the day the gravimeter operators disturb the operations for their movements in the room.

The measurement were taken by Emanuele Biolcati, Claudio Origlia and Alessandro Germak in the days between the 11^{th} and the 15^{th} of November 2013. IMGC-02 were placed in the three sites chosen by the organizers: B5, C2, C3 and in the following the results for each site will be reported.

For each data session, the instrument processed and stored more than 1000 trajectories. Outliers are found by applying the Chauvenet criterion to the estimating parameters such as the vertical gradient, the friction of residual air and to the estimated g value. The final value was extracted by the mean of the acceleration values coming from each drop.

We arrived on the 10^{th} of November at 10 p.m. (UTC), we mounted the whole apparatus and we switched on the vacuum pump system. The night was dedicated to the warm-up phase of the instrument.

Every component of the IMGC-02 was found in the nominal status. The He-Ne laser reaches the nominal equivalent power of 5.6 V. The seismometer period resulted to be of 17.8 s. The pillar to floor height was 73.3 mm.

2.1.1 Site B5

During the first night, the apparatus experienced an oscillation of about 35 μGal. The averaged trajectory residuals after the measurement session are within 8 nm. The time series and the distribution of the g values, the data sets (each correspondent to the average of 50 values), the trajectory fit residuals are reported in figure 2, whilst the figure 3 reports ambient temperature and local barometric pressure acquired at each launch. In table 1 the most important results and parameters are listed ($1\ \mu\text{Gal} = 1 \times 10^{-8}\ \text{m s}^{-2}$).

The measurement uncertainty is summarized in table 3. It includes the instrumental uncertainty reported in table 2.

Only the non-negligible contributions are reported. In the second column, the type of the error is indicated together with its probability distribution: U stays for U shape, *rect* for rectangular one. The degrees of freedom are calculated using the Welch-Satterthwaite formula, whilst the coverage factor comes from the t-Student distribution.

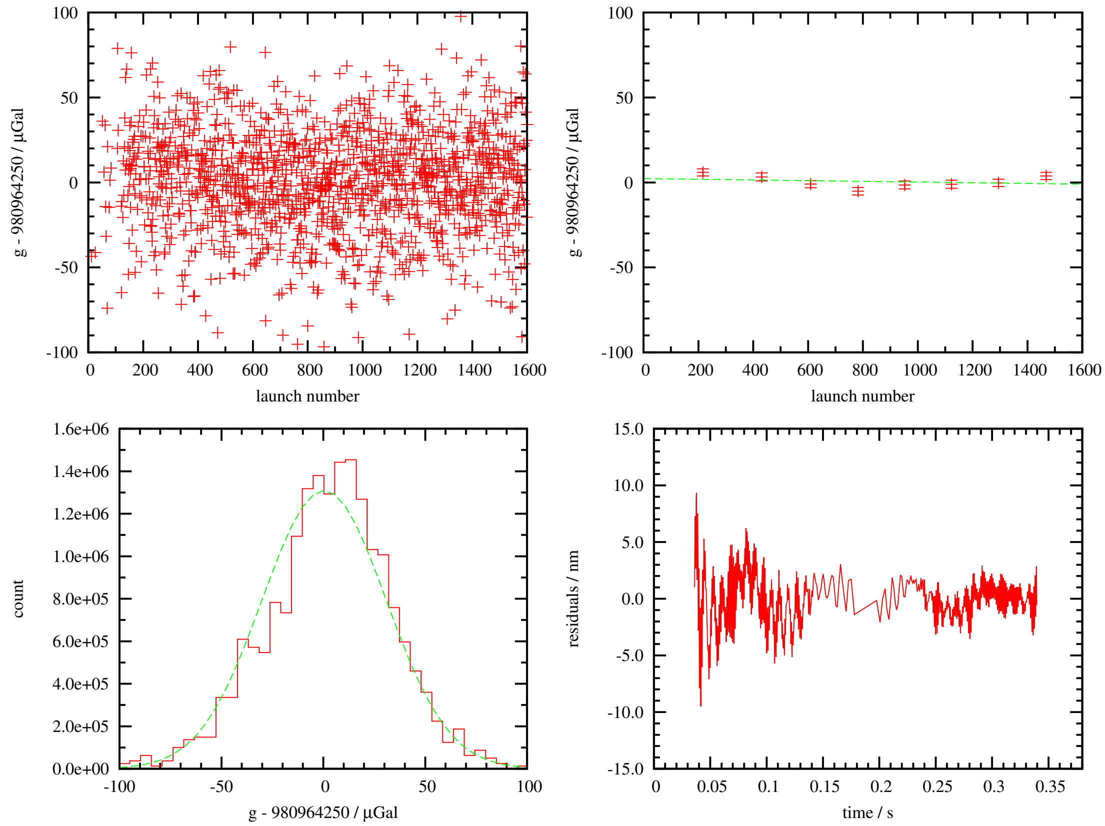

Figure 2: Experimental results for the absolute measurements at the site B5. All and averaged values of g (minus a nominal value for visibility) versus launch number (top). Distribution of the those values with Gaussian fit superimposed and averaged residuals from the fit function to the trajectories (bottom).

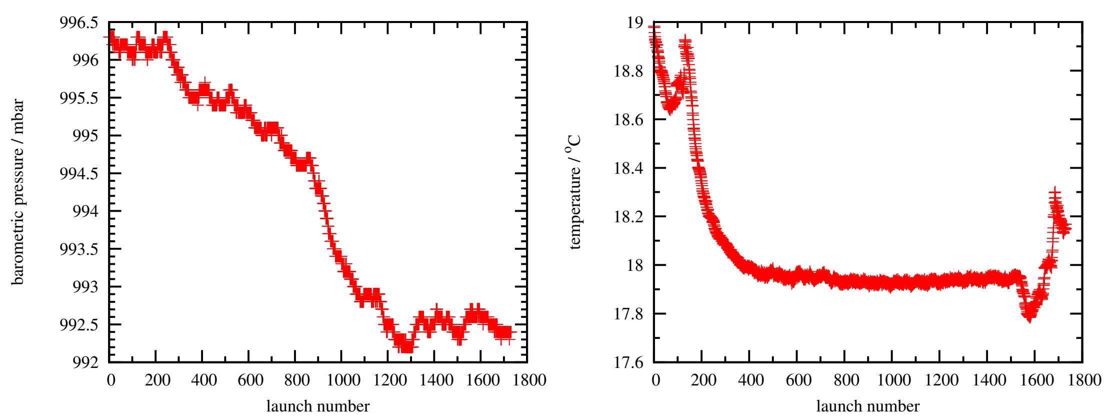

Figure 3: Experimental parameters using for the absolute measurements at the site B5. Barometric pressure and ambient temperature values versus the launch number.

Site information B5	
Data taking start (UTC)	11-11-2013 17:05
Data taking stop (UTC)	12-11-2013 09:06
Geodetic longitude	49.6647 N
Geodetic latitude	6.1528 E
Topographic elevation	295 m
Nominal pressure	978.3 mbar
Pole coordinates in IERS system	(0.074841,0.285789)

Measurement parameters	
Data taking time	16 hours
Event rate	0.03 Hz
Total drift effect	3.0 μGal
Temperature range	(17.8÷19.0) °C
Mean barometric pressure	994.2 mbar

Results	
Accepted/total drops	1519/1731
Standard deviation	30.1 μGal
Standard deviation of the mean	0.8 μGal
Combined uncertainty	4.1 μGal
Vertical gradient	(-267.7±2.0) μGal/m
Corrected mean g value	**980 964 250.2 μGal**
Expanded uncertainty (c.l. 95%)	**8.4 μGal**
Reference height	**0.4709 m**

Processing parameters	
Fitting model	Non-linear, laser modulation
Software	GravisoftPP 2.6
Waveform digitizer sampling freq.	50 MHz
Laser wavelength	632.9912130 nm
Clock frequency	10000000.00092 Hz
Laser modulation frequency	1165.2 Hz
Total rise-and-fall stations	700
Cut upper stations	2
Fringe amplitude threshold	100%
Residual threshold	2000 nm

Table 1: Experimental results at the site B5.

Instrumental uncertainty

x_i	type	corr.	a_i or s_i	$\partial y/\partial x_i$	dof	u_i / μGal
temperature	B - U	0	0.15 μGal	1	10	0.11
laser verticality	B - rect.	0.66 μGal	0.21 μGal	1	15	0.12
laser accuracy	A	0	0.1 μGal	1	30	0.1
beam divergence	A	5.2 μGal	0.52 μGal	1	10	0.52
clock delay	A	0	0.6 μGal	1	30	0.6
reflector balancing	B - rect.	0	0.0001 m	6.3×10^{-4}	15	3.6
reference height	B - rect.	0	0.0005 m	3.0×10^{-6}	30	0.09
self-attraction	A	0.7	0.1 μGal	1	30	0.1
total correction		6.6 μGal				
combined uncert.						3.7 μGal
		degrees of freedom	17			
		confidence level	95%			
		coverage factor	2.1			
		expanded uncertainty	7.9 μGal			

Table 2: Instrumental uncertainty of the IMGC-02. Drag, out gassing, magnetic and electrostatic field, air gap modulation, refraction index, fringe timing and radiation pressure are negligible for the budget uncertainty (1 μGal = 1×10^{-8} m s^{-2}).

Measurement uncertainty at the site B5

x_i	type	corr.	a_i or s_i	$\partial y/\partial x_i$	dof	u_i / μGal
instrumental	A	0	3.7 μGal	1.0	17	3.7
Coriolis force	B - rect.	0	2.8 μGal	1.0	10	1.4
barometric pressure	B - rect.	4.8 μGal	1.0 μGal	1.0	15	0.58
tide	A	-16.3 μGal	0.3 μGal	1.0	15	0.3
ocean loading	A	0	0.2 μGal	1.0	15	0.2
standard dev. mean	A	0	0.8 μGal	1.0	1519	0.8
total correction		-12.8 μGal				
combined uncert.						4.1 μGal
		degrees of freedom	24			
		confidence level	95%			
		coverage factor	2.1			
		expanded uncertainty	8.4 μGal			

Table 3: Final uncertainty for the absolute measurement at the site B5. Floor recoil effect and polar motion correction (0.8 μGal) are negligible for the budget uncertainty. Data taken during the first night are used only.

2.1.2 Site C2

During the first night, the apparatus experienced an oscillation of about 35 μGal. The averaged trajectory residuals after the measurement session are within 8 nm. The time series and the distribution of the g values, the data sets (each correspondent to the average of 50 values), the trajectory fit residuals are reported in figure 4, whilst the figure 5 reports ambient temperature and local barometric pressure acquired at each launch. In table 4 the most important results and parameters are listed (1 μGal $= 1 \times 10^{-8}$ m s^{-2}).

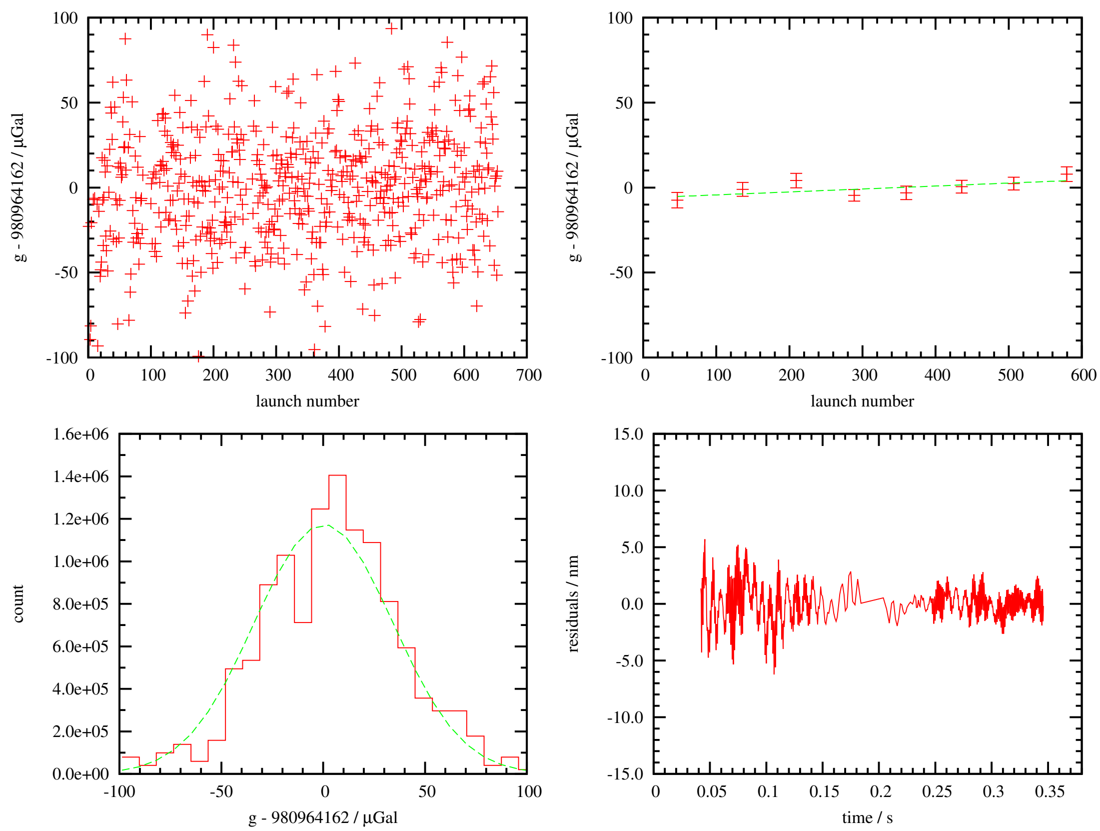

Figure 4: Experimental results for the absolute measurements at the site C2. All and averaged values of g (minus a nominal value for visibility) versus launch number (top). Distribution of the those values with Gaussian fit superimposed and averaged residuals from the fit function to the trajectories (bottom).

The measurement uncertainty is summarized in table 5, using the values coming from the first night. It includes the instrumental uncertainty reported in table 2.

Only the non-negligible contributions are reported. In the third column, the type of the error is indicated together with its probability distribution: U stays for U shape, *rect* for rectangular one. The degrees of freedom are calculated using the Welch-Satterthwaite formula, whilst the coverage factor comes from the t-Student distribution.

Site information C2	
Data taking start (UTC)	13-11-2013 08:09
Data taking stop (UTC)	13-11-2013 13:20
Geodetic longitude	49.6647 N
Geodetic latitude	6.1528 E
Topographic elevation	295 m
Nominal pressure	978.3 mbar
Pole coordinates in IERS system	(0.074841,0.285789)

Measurement parameters	
Data taking time	5.2 hours
Event rate	0.03 Hz
Total drift effect	12.8 μGal
Temperature range	(18.3÷19.4) °C
Mean barometric pressure	997.2 mbar

Results	
Accepted/total drops	597/694
Standard deviation	34.0 μGal
Standard deviation of the mean	1.4 μGal
Combined uncertainty	4.2 μGal
Vertical gradient	(-273.0±1.7) μGal/m
Corrected mean g value	**980 964 162.4 μGal**
Expanded uncertainty (c.l. 95%)	**8.7 μGal**
Reference height	**0.4822 m**

Processing parameters	
Fitting model	Non-linear, laser modulation
Software	GravisoftPP 2.6
Waveform digitizer sampling freq.	50 MHz
Laser wavelength	632.9912130 nm
Clock frequency	10000000.00092 Hz
Laser modulation frequency	1165.2 Hz
Total rise-and-fall stations	700
Cut upper stations	2
Fringe amplitude threshold	100%
Residual threshold	2000 nm

Table 4: Experimental results at the site C2.

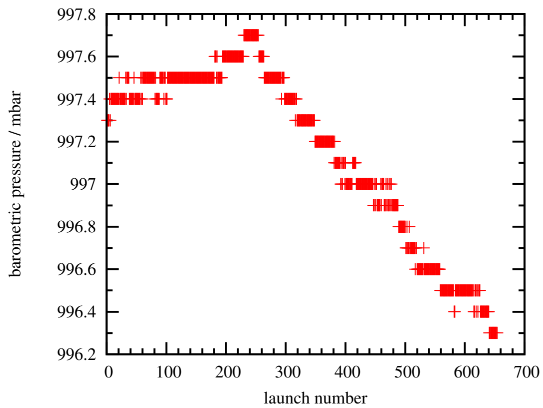

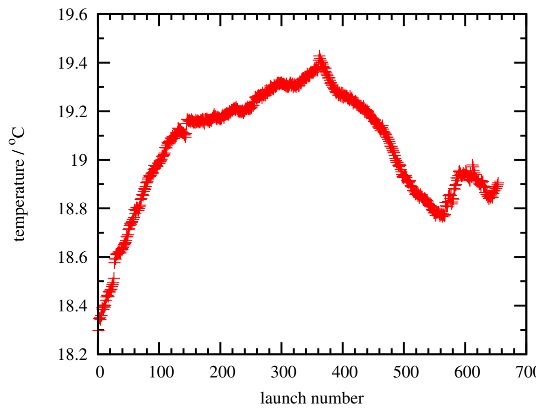

Figure 5: Experimental parameters using for the absolute measurements at the site C2. Barometric pressure and ambient temperature values versus the launch number.

Measurement uncertainty at the site C2

x_i	type	corr.	a_i or s_i	$\partial y/\partial x_i$	dof	u_i / μGal
instrumental	A	0	3.7 μGal	1.0	17	3.7
Coriolis force	B - rect.	0	2.8 μGal	1.0	10	1.6
barometric pressure	B - rect.	5.4 μGal	1.0 μGal	1.0	15	0.58
tide	A	-43.1 μGal	0.3 μGal	1.0	15	0.3
ocean loading	A	0	0.2 μGal	1.0	15	0.2
standard dev. mean	A	0	1.4 μGal	1.0	596	1.4
total correction		-38.5 μGal				
combined uncert.						4.2 μGal
		degrees of freedom	28			
		confidence level	95%			
		coverage factor	2.1			
		expanded uncertainty	8.7 μGal			

Table 5: Final uncertainty for the absolute measurement at the site C2. Floor recoil effect and polar motion correction (0.8 μGal) are negligible for the budget uncertainty.

2.1.3 Site C3

During the first night, the apparatus experienced an oscillation of about 35 μGal. The averaged trajectory residuals after the measurement session are within 8 nm. The time series and the distribution of the g values, the data sets (each correspondent to the average of 50 values), the trajectory fit residuals are reported in figure 6, whilst the figure 7 reports ambient temperature and local barometric pressure acquired at each launch. In table 6 the most important results and parameters are listed (1 μGal $= 1 \times 10^{-8}$ m s^{-2}).

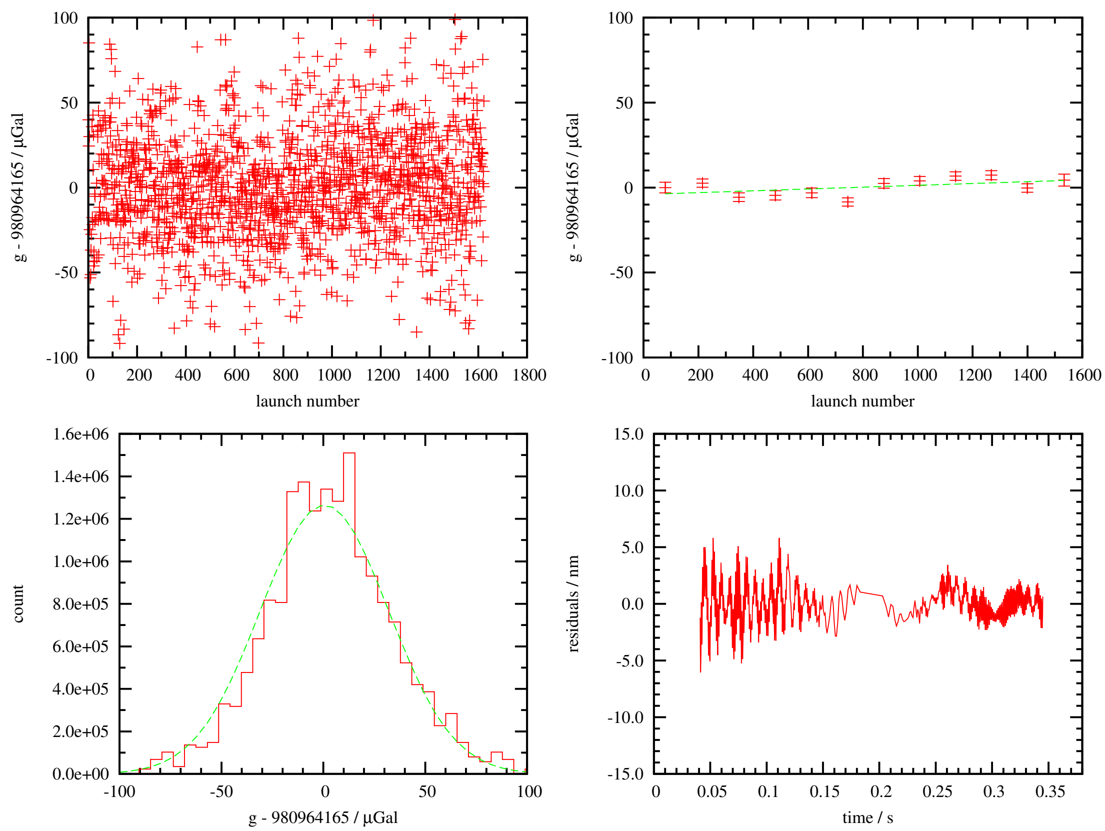

Figure 6: Experimental results for the absolute measurements at the site C3. All and averaged values of g (minus a nominal value for visibility) versus launch number (top). Distribution of the those values with Gaussian fit superimposed and averaged residuals from the fit function to the trajectories (bottom).

The measurement uncertainty is summarized in table 7. It includes the instrumental uncertainty reported in table 2.

Only the non-negligible contributions are reported. In the third column, the type of the error is indicated together with its probability distribution: U stays for U shape, *rect* for rectangular one. The degrees of freedom are calculated using the Welch-Satterthwaite formula, whilst the coverage factor comes from the t-Student distribution.

Site information C3	
Data taking start (UTC)	13-11-2013 17:27
Data taking stop (UTC)	14-11-2013 07:28
Geodetic longitude	49.6647 N
Geodetic latitude	6.1528 E
Topographic elevation	295 m
Nominal pressure	978.3 mbar
Pole coordinates in IERS system	(0.074841,0.285789)
Measurement parameters	
Data taking time	14.5 hours
Event rate	0.03 Hz
Total drift effect	9.2 μGal
Temperature range	(17.9÷19.4) °C
Mean barometric pressure	991.7 mbar
Results	
Accepted/total drops	1581/1624
Standard deviation	31.6 μGal
Standard deviation of the mean	0.8 μGal
Combined uncertainty	4.1 μGal
Vertical gradient	(-271.9±1.0) μGal/m
Corrected mean g value	**980 964 165.4 μGal**
Expanded uncertainty (c.l. 95%)	**8.4 μGal**
Reference height	**0.4805 m**
Processing parameters	
Fitting model	Non-linear, laser modulation
Software	GravisoftPP 2.6
Waveform digitizer sampling freq.	50 MHz
Laser wavelength	632.9912130 nm
Clock frequency	10000000.00092 Hz
Laser modulation frequency	1165.2 Hz
Total rise-and-fall stations	700
Cut upper stations	2
Fringe amplitude threshold	100%
Residual threshold	2000 nm

Table 6: Experimental results at the site C3.

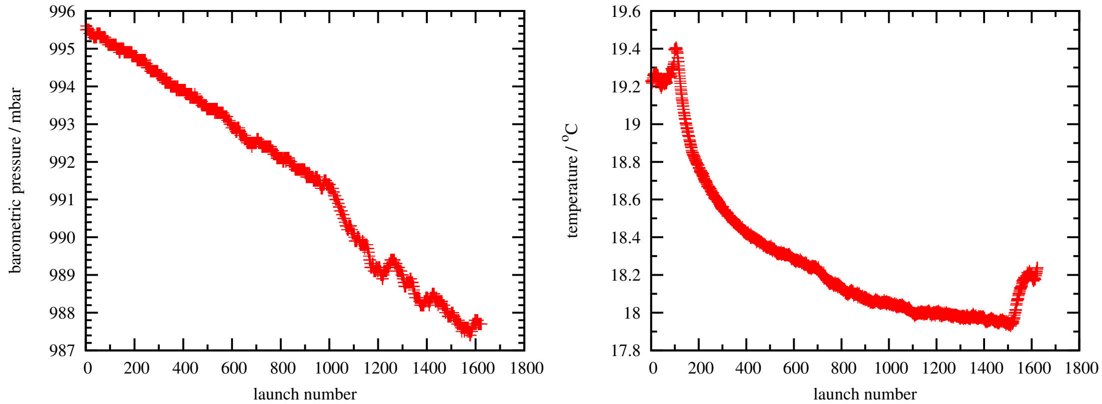

Figure 7: Experimental parameters using for the absolute measurements at the site C3. Barometric pressure and ambient temperature values versus the launch number.

Measurement uncertainty at the site C3

x_i	type	corr.	a_i or s_i	$\partial y/\partial x_i$	dof	u_i / μGal
instrumental	A	0	3.7 μGal	1.0	17	3.7
Coriolis force	B - rect.	0	2.8 μGal	1.0	10	1.6
barometric pressure	B - rect.	0.3 μGal	1.0 μGal	1.0	15	0.58
tide	A	0.8 μGal	0.3 μGal	1.0	15	0.3
ocean loading	A	0	0.2 μGal	1.0	15	0.2
standard dev. mean	A	0	0.7 μGal	1.0	1580	0.7
total correction		1.2 μGal				
combined uncert.						4.1 μGal
		degrees of freedom	24			
		confidence level	95%			
		coverage factor	2.1			
		expanded uncertainty	8.4 μGal			

Table 7: Final uncertainty for the absolute measurement at the site C3. Floor recoil effect and polar motion correction (0.8 μGal) are negligible for the budget uncertainty.

3 Conclusion

The measurements of the free-fall acceleration g requested for the active participation to the International Comparison of Absolute Gravimeters were performed. The IMGC-02 absolute gravimeter presented a good performance, with negligible drift effects and no accidental misalignment. For each point of measurement, a dataset allows us to extract the g value with the nominal uncertainty.

The final values are the following ones:

- for site B5: $g = (\ 980\ 964\ 250.2 \pm 8.4\ )\ \mu\text{Gal}$ @ $h_{\text{ref}} = 470.9$ mm
- for site C2: $g = (\ 980\ 964\ 162.4 \pm 8.7\ )\ \mu\text{Gal}$ @ $h_{\text{ref}} = 482.2$ mm
- for site C3: $g = (\ 980\ 964\ 165.4 \pm 8.4\ )\ \mu\text{Gal}$ @ $h_{\text{ref}} = 480.5$ mm

where the expanded uncertainty is calculated using the coverage factor for a confidence level of 95% .

References

[1] D'Agostino G, Desogus S, Germak A, Origlia C, Quagliotti D, Berrino G, Corrado G, d'Errico V and Ricciardi G, *The new IMGC-02 transportable absolute gravimeter: measurement apparatus and applications in geophysics and volcanology*, Ann. Geophys. **51** (2008) 3949

[2] Biolcati E, Desogus S, Mazzoleni F, Origlia C, Vitiello F, *Modifiche apportate al gravimetro assoluto IMGC-02*, INRiM - RT 37/2012

[3] Germak A, Desogus S, Origlia C, *Interferometer for the IMGC rise-and-fall absolute gravimeter*, Metrologia, Special issue on gravimetry, Bureau Int Poids Mesures, BIPM, Pavillon De Breteuil, F-92312, Svres Cedex, France, 2002, Vol. 39, Nr. 5, pp. 471-475

[4] D'Agostino G, Germak A, Desogus S, Barbato G, *A Method to Estimate the Time-Position Coordinates of a Free-Falling Test-Mass in Absolute Grvimetry*, Metrologia Vol. 42, No. 4, pp. 233-238, August 2005.

[5] *Evaluation of measurement data Guide to the expression of uncertainty in measurement*, JCGM 100:2008 (GUM 1995 with minor corrections)

[6] Biolcati E, Svitlov S, Germak A, *Self-attraction effect and correction on three absolute gravimeters*, Metrologia **49** (2012) 560566